Доклади на Българската академия на науките
Comptes rendus de l'Académie bulgare des Sciences
Tome 64, No 4, 2011

MATHEMATIQUES
Modèles mathématiques

NUMERICAL STUDY OF THE STATIC CONTACT ANGLE HYSTERESIS IN THE PRESENCE OF PERIODIC DEFECTS

Stanimir Iliev, Nina Pesheva

(*Submitted by Corresponding Member S. Radev on December 6, 2010*)

Abstract

Here we study numerically the static hysteresis interval of the observable contact angles (CAs) for the dipped plate geometry, where the immersed in a tank of liquid vertical smooth solid plate has doubly periodic heterogeneous surface. The two types of heterogeneity domains have sharp borders between them which is a case qualitatively different from the case when the surface tension of the plate varies smoothly. The hysteresis interval is obtained on the basis of exact solutions for the meniscus shape and position without any assumptions for small curvatures of the meniscus deformations caused by the heterogeneities on the plate. We use two definitions for the receding and advancing CAs. The first definition defines the minimal and the maximal possible averaged cosine of the CA among all possible positions of the plate with respect to the liquid level, while the second definition defines the averaged advancing and receding CAs over different realizations of the position of the defects on the plate relative to the liquid level. In the second definition the receding CAs can be considered as effective CAs for very small values of the plate velocity for immersing and withdrawing plate correspondingly. We find that the second hysteresis interval is contained in the first.

Key words: capillarity, contact angle, heterogeneous surface, hysteresis
2000 Mathematics Subject Classification: 76B45, 76M30

1. Introduction. Wetting of a liquid on non-ideal solid surfaces is still an open problem of general interest. The study of this problem is very important, since most of the real surfaces appearing in nature, in the laboratories, and in the

The first author has received financial support from the National Scientific Fund of Bulgaria under Grant No DO 02 115/08.

different technological processes are not ideal – they are rough and heterogeneous, have finite rigidity, etc. It is very important to establish a relation between the heterogeneity parameters and the behaviours of the observable contact line (CL) and the observable contact angle (CA). We focus on the effect of a flat substrate with chemical disorder on the observable advancing and receding CAs. Here, we obtain numerically metastable shapes $\Sigma_{lf} = \{x, y, z(x, y)\}$ of the liquid meniscus in contact with a vertical heterogeneous plate partially immersed in a tank of liquid as shown in Fig. 1(a). Studies of wetting in the case of flat but chemically heterogeneous substrates have been carried out mainly for regularly patterned surfaces. Joanny and de Gennes [1] studied the effect of a single defect on the values of θ^r_{eq}, θ^a_{eq} (a – advancing, r – receding) for small deformations of the meniscus z_x^2, $z_y^2 \ll 1$. For the same system and assumptions for the shape of the meniscus, Schwartz and Garoff [2] determined the magnitude of the hysteresis interval in the case of doubly periodic heterogeneous plates. Recently, the case of randomly heterogeneous surface was studied by David and Neumann [3] for the dipped plate geometry, using the corrugation energy approximation of the plate defects of Ref. [1]. Solutions in Refs [1–3] are available for small deformations of the meniscus z_x^2, $z_y^2 \ll 1$. Currently it is of interest to obtain the hysteresis interval on the basis of exact solutions for the meniscus shape and position without any assumptions for small curvatures of the meniscus deformations caused by the heterogeneities on the plate and that is the objective of the present study.

2. Problem formulation. We are interested in the meniscus, which forms when a vertical heterogeneous (but smooth) solid plate is partially immersed in a tank of liquid. One of the plate faces is described with Cartesian coordinates (y, z)

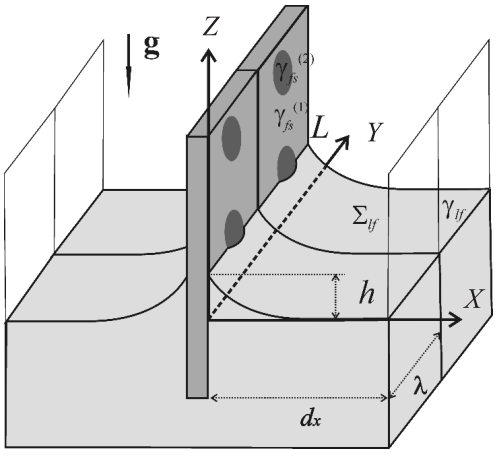

Fig. 1(a). Schematic drawing of the considered system

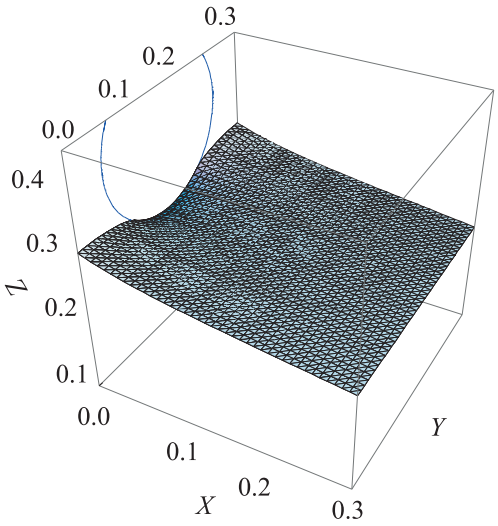

Fig. 1(b). A part of the approximated meniscus surface close to the plate

where the y-axis is horizontal and the z-axis is directed upwards as shown in Fig. 1(a). The liquid free surface is denoted by Σ_{lf}, and the CL the liquid meniscus forms with the solid surface by L, where $\Sigma_{lf} = \{x, y, z(x, y)\}$ and $L = \{y, h(y)\}$.

The distance between the plate and the bath wall opposite to the plate is denoted by d_x and the width of the plate – by d_y. We focus here on the case when the surface of the plate consists of two kinds of homogeneous domains $\Sigma^{(i)}$ $(i = 1, 2)$ with sharp borders between them (let us note that this case is qualitatively different from the case when the surface tension of the solid plate varies smoothly). Inside the domains, the surface tensions are (solid–vapour) $\gamma_{sl}^{(i)}$ and (solid–fluid) $\gamma_{sf}^{(i)}$. The domain pattern is considered to be double-periodical with a spatial period λ in both directions (z and y). In the capillary theory the free energy U of the system is

$$(1)\quad U = \int\limits_{\Sigma_{lf}} \gamma_{lf} d\,\Sigma_{lf} + \sum_{i=1,2} \left(\int\limits_{\Sigma^{(i)}} \gamma_{sf}^{(i)} d\,\Sigma + \int\limits_{\Sigma^{(i)}} \gamma_{sl}^{(i)} d\,\Sigma \right) + \int\limits_{\Omega_l} \rho_l\, U_{gr} d\,\Omega_l + \int\limits_{\Omega_f} \rho_f\, U_{gr} d\,\Omega_f,$$

where the volume and the density of the liquid in the bath and the ambient fluid are denoted by Ω_l, ρ_l and Ω_f, ρ_f, respectively, and $U_{gr} = gz$ is the potential of the gravitation field. The last term in (1) is very small and is usually neglected. The metastable static shape of the meniscus is determined [4] by the condition

$$(2)\qquad \delta\, U \geq 0,$$

for any possible variation of the points belonging to the meniscus Σ_{lf}. The problem can be made dimensionless by expressing the lengths in terms of the capillary length $l_c = (\gamma_{sl}/\rho_l g)^{1/2}$. From now on we shall use the dimensionless variables and for simplicity we shall keep the same notation. Our study here focuses on a pattern studied previously in [5]. It consists of domains $\Sigma^{(2)}$ characterized by CA $\theta^{(2)} = 110^\circ$ $(\cos\theta^{(i)} = (\gamma_{sf}^{(i)} - \gamma_{sl}^{(i)})/\gamma_{lf})$, which are circles of radius $a = 0.1$ ordered on a square lattice with a period $\lambda = 0.3$. The rest of the plate is domain $\Sigma^{(1)}$ with CA $\theta^{(1)} = 70^\circ$.

We are interested also in the amplitude F of the z-component of the wetting force exerted by the meniscus on the Wilhelmy plate

$$(3)\qquad F = \gamma_{lf} \int\limits_{L} \cos\theta\ (L)\, \vec{z} \cdot \vec{n} dl = \gamma_{lf} \int\limits_{0}^{d_y} \cos\theta\,(h\,(y)\,, y)\ dy.$$

$F/(d_y \gamma_{lf})$ is used to define [5, 6] the spatially averaged cosine $\langle\cos\theta\rangle = F/(d_y\gamma_{lf})$ of the CA.

3. Numerical algorithm. Here, we give only a very concise description of the numerical procedure. It consists of parts described in detail in Refs [4, 7].

We take here $d_x = 10$. A part of the meniscus of width λ along y-axes and length d_x (in x-direction) is approximated by a set of triangles with vertex points $R_{ij} = R[x_i, y_i, z(x_i, y_i)]$; $i = 1, \ldots, 800$; $j = 1, \ldots, 50$ (see Fig. 1(b), where a part of the approximated meniscus surface, close to the plate, is shown). Periodic boundary conditions are imposed in y-direction. The change of the meniscus shape and the CL is determined by analysis of the change in energy $\Delta U(R_{ij})$, calculated for small virtual displacements ΔR_{ij} of the nodes R_{ij}. We find the metastable equilibrium shapes of the liquid meniscus by applying a minimization procedure (based on the local variation approach). The obtained equilibrium state depends, if it is not unique, on the initial state, from which the minimization was started.

4. Numerical results. The presence of heterogeneity leads to a set of different possible equilibrium states of the meniscus. A number of equilibrium meniscus states appear for each relative position of the heterogeneity pattern with respect to the liquid level. The relative position of the pattern is given by the height $H \in [0, \lambda)$ of the centres of a row of circles with respect to the liquid level far away from the plate. For every value of H, there is a set of equilibrium liquid meniscus states and, respectively, a set of corresponding CLs. Here, we find the equilibrium meniscuses with the highest and lowest possible averaged heights $h^+(y, H_i)$, $\{h^-(y, H_i)\}$ of the CLs among all possible CLs of the equilibrium meniscuses. These two solutions define $\langle \cos\theta \rangle_r (H)$ and $\langle \cos\theta \rangle_a (H)$ which are the biggest and the smallest value for the averaged cosine of the CA among all possible values appearing from all metastable equilibrium shapes of the liquid meniscus. For the cosines of the $\theta^a_{eq}, \theta^r_{eq}$ the following definitions will be considered:

$$\cos\theta^a_{eq} = \min_{0 \le H < \lambda} \langle \cos\theta \rangle_a (H); \quad \cos\theta^r_{eq} = \max_{0 \le H < \lambda} \langle \cos\theta \rangle_r (H) \tag{4}$$

and

$$\cos\overline{\theta^a_{eq}} = \langle \langle \cos\theta \rangle_a (H) \rangle_{(H)}; \quad \cos\overline{\theta^r_{eq}} = \langle \langle \cos\theta \rangle_r (H) \rangle_{(H)}. \tag{5}$$

The first definition (4) defines the minimal and the maximal possible averaged cosine of the CA among all possible positions of the plate, while definition (5) defines the averaged advancing and receding CAs over all different realizations of the position of the defects on the plate relative to the liquid level far away from the plate. According to this second definition the advancing and the receding CAs can be considered as effective CAs for very small values of the plate velocity for immersing and withdrawing plate, correspondingly. Because of this $\overline{\theta^a_{eq}}$ and $\overline{\theta^r_{eq}}$ can be considered as limits of the static hysteresis interval obtained by the dynamic approach [8].

Taking into account that all the heights $h(y)$ of the possible equilibrium CLs lie in the interval $[h_-, h_+]$, where $h_\pm = \pm(2 - 2\sin\theta^{(1)})^{1/2}$, for obtaining the

equilibrium shapes of the liquid meniscus having CLs with the highest and the lowest average heights $h^+(y, H_i)$, $h^-(y, H_i)$, we start the numerical algorithm (for every value of H) with initial meniscus shapes having horizontal CL with the highest possible averaged h_+ and lowest possible h_- heights, respectively. We show in Figs 2(a) and 2(b), respectively, the obtained equilibrium CLs with $h^+(y, H_i)$, $h^-(y, H_i)$ for 20 different positions of the heterogeneity pattern with respect to the liquid level characterized by $H_i = i\lambda/20$, $i = 0, 1, \ldots, 19$ in a reference system attached to the tank of liquid (note that $H_0 \equiv H_{20}$). These 20

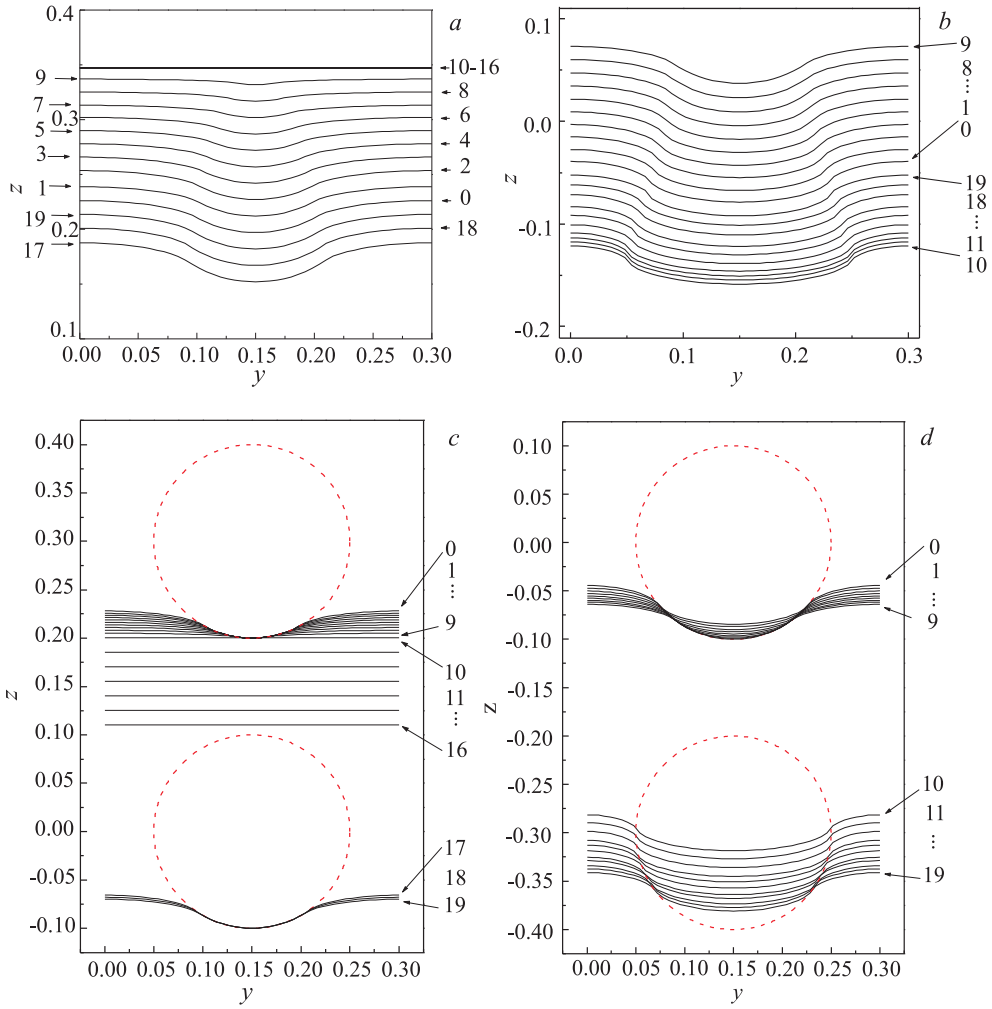

Fig. 2. Equilibrium CLs with highest average height are shown in (a) and (c) and with the lowest average height in (b) and (d) for 20 different positions of the heterogeneity pattern. The CLs shown in (a) and (b) are in a reference system attached to the tank of liquid. These CLs are shifted in such a way so that their relative position with respect to the circular defects is seen in (c) and in (d), respectively

different positions of the heterogeneity pattern approximate uniformly all possible different positions of the heterogeneous plate with respect to the liquid level far away from the plate. The contact lines from these Figures are shown in Figs 2(c) and 2(d), respectively, shifted in such a way so that their relative positions with respect to the circular defects are seen. The numbering of the contact lines corresponds to the index i, defining the relative position of the heterogeneity pattern with respect to the liquid level H_i. The specific choice of $\theta^{(1)}$ and $\theta^{(2)}$ as well as of the specific type of heterogeneity pattern lead to difference in the shapes and the positions of the CLs belonging to the sets of CLs $\{h^+(y, H_i)\}$ and $\{h^-(y, H_i)\}$.

Equilibrium CLs with highest average height: For H_0 =0 the initial CL with height h_+ passes through the upper parts of the circular defects belonging to the second row of defects above the liquid level. Since in the minimization procedure the CL starts to slide down, until the equilibrium state is attained, which is in fact achieved when the CL reaches and sticks to the lower border of the defect. The same behaviour of the CL is observed (since again the initial CL passes through the second row of defects above the liquid level) for the next nine different positions of the heterogeneity pattern with respect to the liquid level $H_i = i\lambda/20$, $i = 0, 1, \ldots, 9$. However, when the position of the heterogeneity pattern with respect to the liquid level is such that the initial CL lies in the band of material where $\theta^{(1)} = 70^\circ$, between two rows of defects, then it appears that then the equilibrium CL with the highest possible height is reached and this is the case for all heights $H_i = i\lambda/20$, $i = 10, \ldots, 16$. For all these positions of the heterogeneity pattern with respect to the liquid level, the final equilibrium CL is one and the same.

Equilibrium CLs with the lowest average height: The situation is quite the opposite when studying the set of contact lines $\{h^-(y, H_i)\}$ shown in Fig. 2 (b), (d). The parts of the initial CL which are outside the circular defects are trying to reach the height corresponding to $\theta^{(1)} = 70^\circ$. At the same time, the parts of the CL on the circular spots are trying to reach $\theta^{(2)} = 110^\circ$. During the minimization process the CL relaxes until outside the spots a CA of value $\theta^{(1)}$ is attained. In this case there are no parts of the CL which stick to the border of the defects as in the $\{h^+(y, H_i)\}$ case. In the minimization process it might happen that the CL needs to pass through several rows of defects before the equilibrium state is attained.

The specific behaviour of the sets of CLs $\{h^+(y, H_i)\}$ and $\{h^-(y, H_i)\}$ is reflected also on the values of the local equilibrium CAs $\theta(y, i)$. In the case $\{h^-(y, H_i)\}$, since there are no parts of the CL stuck to the border of defects, one has that $\theta(y, i)$ is $\theta^{(2)}$ on the parts of the CL which are inside the spots and $\theta^{(1)}$ on the parts of the CL which are outside the spots. In the case $\{h^+(y, H_i)\}$, $\theta(y, i)$ is again $\theta^{(1)}$ on the parts of the CL which are outside the spots, but on the parts of the CL which are stuck to the border of the defects $\theta(y, i)$ is in the interval

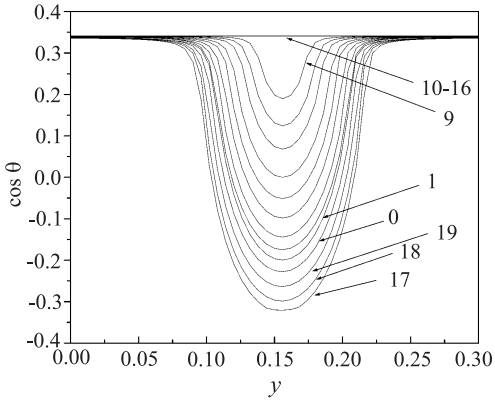

Fig. 3. Local equilibrium cosine of the CA θ as function of y corresponding to the equilibrium contact lines shown in Fig. 2(a)

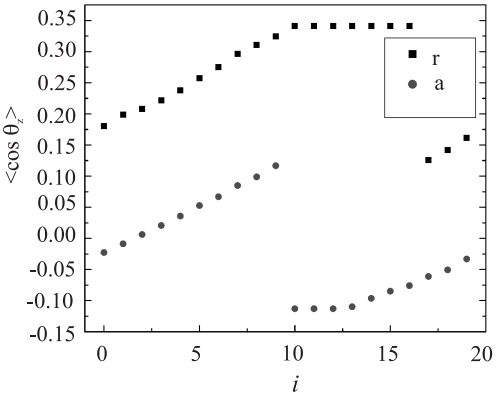

Fig. 4. Cosine of the receding (solid squares) and advancing (solid circles) CA as function of position of the pattern H_i with respect to the liquid level

$[\theta^{(1)}, \theta^{(2)}]$. $\theta(y, i)$ are shown in Fig. 4 for the CLs shown in Fig. 2(a). From the results for the CAs it is quite easy to obtain $\langle \cos\theta \rangle_a(H)$ and $\langle \cos\theta \rangle_r(H)$ for given value of H. These results are shown in Fig. 3. From the results shown in Fig. 4 one finds that (using the first definition of advancing and receding CAs – Eq. (4)) $\theta^a_{eq} = 96.49^\circ$ and $\theta^r_{eq} = 70.05^\circ$. If one uses the second definition (Eq. (5)) one gets $\overline{\theta^a_{eq}} = 90.86^\circ$ and $\overline{\theta^r_{eq}} = 75.5^\circ$, respectively. The obtained values for $\overline{\theta^a_{eq}}$ and $\overline{\theta^r_{eq}}$ practically coincide with the ones obtained in [8] in the framework of the Contact Line Dissipation Approach effective contact angles of 90° and 76.5° for $|u| \to 0$ where u is the plate velocity.

In Reference [2] the Straight CL (SCL) approximation $\cos\theta^r_{eq}(SCL)$ and $\cos\theta^a_{eq}(SCL)$ for $\cos\theta^a_{eq}$ and $\cos\theta^r_{eq}$ are proposed. For the heterogeneity pattern we consider here, it is obvious that $\cos\theta^r_{eq}(SCL) = \cos 70^\circ$ and $\cos\theta^a_{eq}(SCL) = 0$. In this case the difference between Straight CL approximation result $\cos\theta^a_{eq}(SCL)$ and the exact solution for the advancing CA $\cos\theta^a_{eq}$ is quite big $\sim 6.5^\circ$. For the receding CA the contact line is a straight line and one has $\cos\theta^r_{eq}(SCL) \approx \cos\theta^r_{eq}$.

In Reference [3] the numerical studies show that the following relation between Cassie's angle θ_c and the receding θ^r_{eq} and advancing CA θ^a_{eq} holds $\cos\theta_c = (\cos\theta^r_{eq} + \cos\theta^a_{eq})/2$. We find that this relation holds also here for the considered heterogeneous plate using first and second definitions of advancing and receding CAs. As one can see from Fig. 4 the following relation $\cos\theta_c = (\langle \cos\theta \rangle_r(H) + \langle \cos\theta \rangle_a(H))/2$ does not hold for every H.

As one can see from (4) and (5) $[\overline{\theta^r_{eq}}, \overline{\theta^a_{eq}}] \subset [\theta^r_{eq}, \theta^a_{eq}]$. In this case the difference between the corresponding angles is $\sim 5.5^\circ$. Taking into account that $\overline{\theta^r_{eq}}$ and $\overline{\theta^a_{eq}}$ can be interpreted as effective CAs for very small values of the plate velocity for withdrawing and immersing plate, correspondingly, then this explains the

difference in the CA hysteresis intervals obtained using the static and the dynamic approach [9]. The intervals of contact angles $[\theta_{eq}^r, \overline{\theta_{eq}^r}]$, $[\overline{\theta_{eq}^a}, \theta_{eq}^a]$ can be considered as metastable static CA, which form when passing from dynamics to statics. Such intervals are observed experimentally in [10].

REFERENCES

[1] Joanny J. F., P. G de Gennes. J. Chem. Phys., **81**, 1984, 552–562.
[2] Schwartz L. W., S. Garoff. Langmuir, **1**, 1985, 219–230.
[3] David R., A. W. Neumann. Langmuir, **26**, 2010, 13256–13262.
[4] Iliev S., N. Pesheva. Langmuir, **19**, 2003, 9923–9931.
[5] Nikolayev V. S. J. Phys.: Condens. Matter., **17**, 2005, 2111–2119.
[6] Della Volpe C., D. Maniglio, S. Siboni, M. Morra. Oil & Gas Science and Technology – Rev. IFP, **56**, 2001, 9–22.
[7] Iliev S., N. Pesheva, V. Nikolayev. Phys. Rev. E, **78**, 2008, 021605.
[8] Iliev S., N. Pesheva, V. Nikolayev. 11th National Congress on Theoretical and Applied Mechanics, Borovets, Bulgaria, 2–5 September 2009. ID:154-307-1-PB.
[9] Dussan V. E. B. Ann. Rev. Fluid Mech., **11**, 1979, 371–400.
[10] Berejnov V. V., R. E. Thorne. Phys. Rev. E, **72**, 2007, 066308.

Institute of Mechanics
Bulgarian Academy of Sciences
Acad. G. Bonchev Str., Bl. 4
1113 Sofia, Bulgaria
e-mail: stani@imbm.bas.bg
nina@imbm.bas.bg